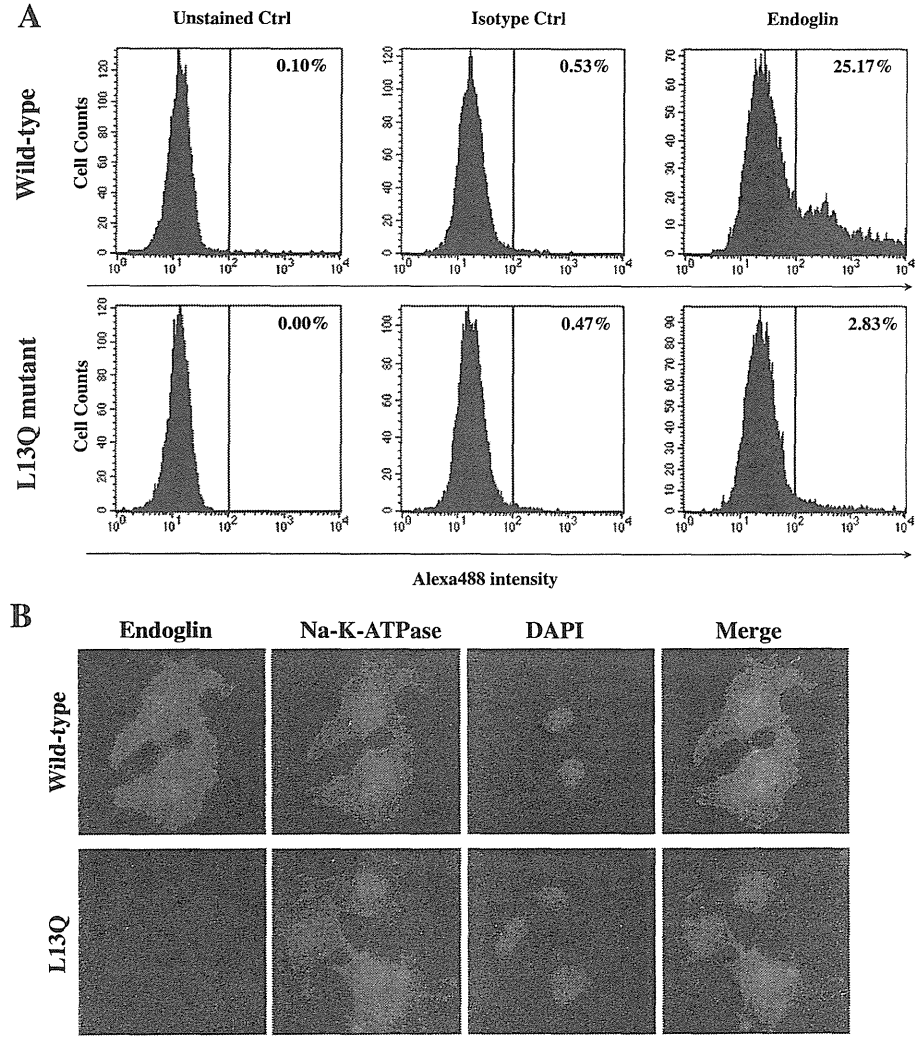


**Fig. 3. Detection of cell surface recombinant endoglins expressed in COS-1cells.** COS-1 cells were transiently transfected with pL-ENG$^{WT}$ or pL-ENG$^{L13Q}$, and analyzed for the cell-surface expression of recombinant endoglins by flow cytometry (A) and immunofluorescence microscopy (B). **A**: Flow cytometry analyses for recombinant endoglins using anti-endoglin antibody. The X-axis indicates Alexa488 fluorescence intensity (recombinant endoglins), and the Y-axis, cell number. Percentages of positive cells in the whole cell population are shown in the upper right corner of each histogram. The upper column shows the results of pL-ENG$^{WT}$-transfected COS-1 cells and the lower column, those of pL-ENG$^{L13Q}$-transfected COS-1 cells. Similar results were obtained in three independent experiments. **B**: Immunofluorescence microscopy for recombinant endoglins and membrane marker Na-K-ATPase. COS-1 cells were transfected with 0.5 μg of pL-ENG$^{WT}$ or pL-ENG$^{L13Q}$. Localization of endoglins and the ER was shown with anti-endoglin antibody (green) and anti-alpha1sodium-potassium ATPase antibody (red), respectively. The images were merged to represent the co-localization of both molecules as yellow signals.

HHT1 [13]. It is reported that endothelial cells lacking endoglins lead to significant angiogenic abnormalities [5], which supports the fundamental roles of endoglin in the correct tuning of physiological effects mediated by TGF-β in endothelial cells [27].

In this study, we investigated the molecular basis of HHT in a Japanese patient, and identified a novel missense mutation in the *ENG* gene (c.38 T>A, p.Leu13Gln), located in the hydrophobic core of the endoglin signal peptide. We conducted PCR-RFLP to detect the c.38 T>A in *ENG*, and confirmed the heterozygosity of the variation in samples of the proband as well as an affected sister, but did not find it in any samples from healthy volunteers (data not shown). These results suggested the c.38 T>A transversion in *ENG* to be a causative mutation of HHT in this patient. There are some reports of missense mutations in the endoglin signal peptide, 3 start codon alterations (p.Met1Thr, p.Met1Arg and p.Met1Val) [3,28,29] and 3 internal part codon alterations (p.Thr5Met, p.Leu8Pro and p.Ala11Asp) [30-32], but their molecular basis has yet to be investigated in detail.

Signal peptides range in size from 15 to 30 amino acids, and their primary sequences are extremely heterogeneous [33]. However, they typically have three essential conserved regions, an amino-terminal positively charged region (n-region), a central hydrophobic part (h-region), and a more polar carboxy-terminal domain (c-region) [34]. The hydrophobic core of seven to fifteen amino acids in the h-region is thought to be critical for co-translational processing into a mature protein [33,35]. This is the first report of a missense mutation at 13Leu in the h-region of the endoglin signal peptide, which is highly conserved in amino acid sequence among species (Fig.6). Therefore, the substitution of the hydrophobic 13Leu with a polar Gln might have a major influence on the structure and function of the endoglin signal peptide.

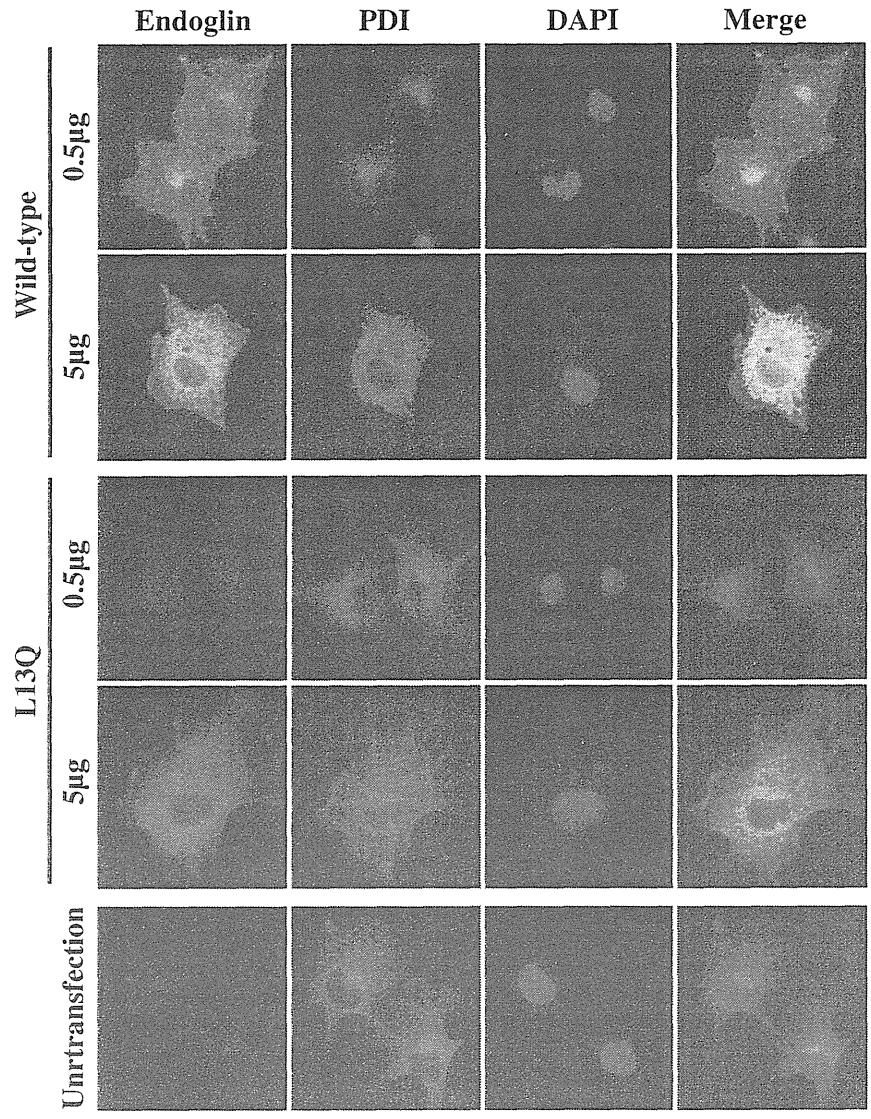


**Fig. 4. Intracellular localization of recombinant endoglins.** Immunofluorescence staining analyses were performed for the COS-1 cells transiently transfected with 0.5 μg or 5 μg of pL-ENG$^{WT}$ or pL-ENG$^{L13Q}$. Localization of endoglins and the ER was shown with anti-endoglin antibody (green) and anti-PDI antibody (red), respectively. The images were merged to represent the co-localization of both molecules as yellow signals. Data for untransfected cells are also shown at the bottom.

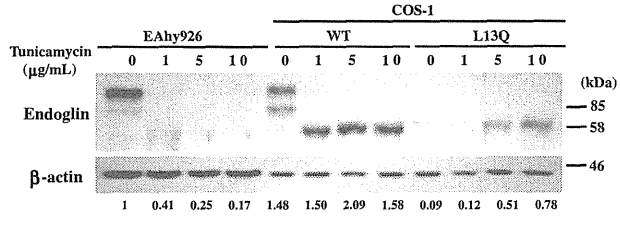


**Fig. 5. Effects of tunicamycin treatment on recombinant endoglins.** COS-1 cells were transiently transfected with pL-ENG$^{WT}$ or pL-ENG$^{L13Q}$, and subsequently treated with 1 to 10 μg/mL tunicamycin for 24 hr. Whole cell lysates from tunicamycin-treated cells as well as from untreated cells were separated by 10% SDS-PAGE under reducing conditions followed by Western blotting. The tunicamycin-treated EAhy926 cells were also analyzed as positive controls. The relative intensity of each endoglin band against the β-actin band was shown in the bottom (that of endogenous endoglin band of the EAhy926 cell is 1).

To examine effects of the L13Q mutation on the structure and function of endoglin, we performed transient expression experiments for the recombinant endoglins in COS-1 cells. In Western blotting under reducing conditions, the wild-type recombinant endoglins were expressed as mainly 2 monomers (a fully processed 90 kDa and partially glycosylated 80 kDa form) as reported previously [36], whereas the L13Q mutant seemed to be expressed as a non-glycosylated precursor monomer (60 kDa). In Western blot analyses under non-reducing conditions, the wild-type recombinant endoglins appeared to be expressed as homodimers, whereas the L13Q mutant remained as a non-glycosylated precursor. It was speculated that the L13Q mutation might impair post-translational processing of endoglin such as glycosylation and dimerization, probably due to a destroyed function of the signal peptide. Flow cytometry and immunofluorescent microscopy analyses of the recombinant endoglins

| Species | Amino Acid Sequence of Signal Peptide (1 10 20; 13) |
|---|---|
| Homo sapiens | MDRGTLPLAVALLLASCSLSPTSLA |
| Pango abelii (orangutan) | MDRGTLPLAVALLLASCSLSPTSLA |
| Equus caballus (horse) | MDRGALPLVVALLLAVCSLSPTSLA |
| Bos taurus (cattle) | MDRGVLCQAMALLLVVCSLSPTSLA |
| Sus scrofa (wild boar) | MDRGVLPQAMALLLAVCSFCPTAGL |
| Mus musculus (mouse) | MDRGVLPLEITLLFVIVSFVPTSLA |
| Rattus norvegicus (rat) | MDRGMLPLVITLLLVIVSFVPTSLA |
| Gallus gallus (chicken) | MCRFSSPLLPLLLALLGPPDPAPAE |

**Fig. 6. Comparison of amino acid sequence of endoglin signal peptide across species.** The amino acid sequences of endoglin signal peptides across diverse species were aligned. Open boxes denote identical amino acids between human endoglin and endoglins from other mammalian species. 13Leu (bold letters **L** in the shaded boxes) is conserved in all species.

also demonstrated that the wild-type endoglins were expressed on the cell surface, but the L13Q mutant was not. These results suggested that the L13Q mutation might severely impair endoglin expression on the cell surface.

To assess the distribution of the recombinant endoglins in the cells, we performed immunofluorescent staining for the wild-type and the L13Q mutant transiently expressed in COS-1 cells, together with staining for ER. We observed that the wild-type endoglin co-localized with ER, but the L13Q mutant did not. In addition, the immunofluorescent pattern of the ER in the COS-1 cells transfected with high amount of pL-ENG$^{WT}$ was different from that in the untransfected cells as well as the pL-ENG$^{L13Q}$-transfected cells, probably due to over-expression of the wild-type recombinant endoglin leading to an excess of protein processing in the ER lumen, that is an ER stress. Overexpression of the wild-type endoglin might cause an ER stress, but not that of the L13Q mutant. Tunicamycin, which blocks the initial step of glycosylation in the ER [37], would affect the expression of wild-type endoglin. In fact, we observed that the wild-type recombinant endoglin in the tunicamycin-treated cells was as small as the L13Q mutant, which showed no difference in size on tunicamycin treatment. These results suggested that the L13Q mutant would not enter into the ER, not undergo correct processing, such as glycosylation, and be retained in the cytoplasm.

Glycosylation is one of the post-translational modifications to often need for crucial functions of the proteins, and incorrect processed proteins may be degraded by the normal quality control system in the protein biosynthesis. Interfering with glycosylation dramatically decreased the stability of endogenous endoglin of EAhy926 cells (Fig. 5). However, it did not seem to affect stability of overexpressed wild-type

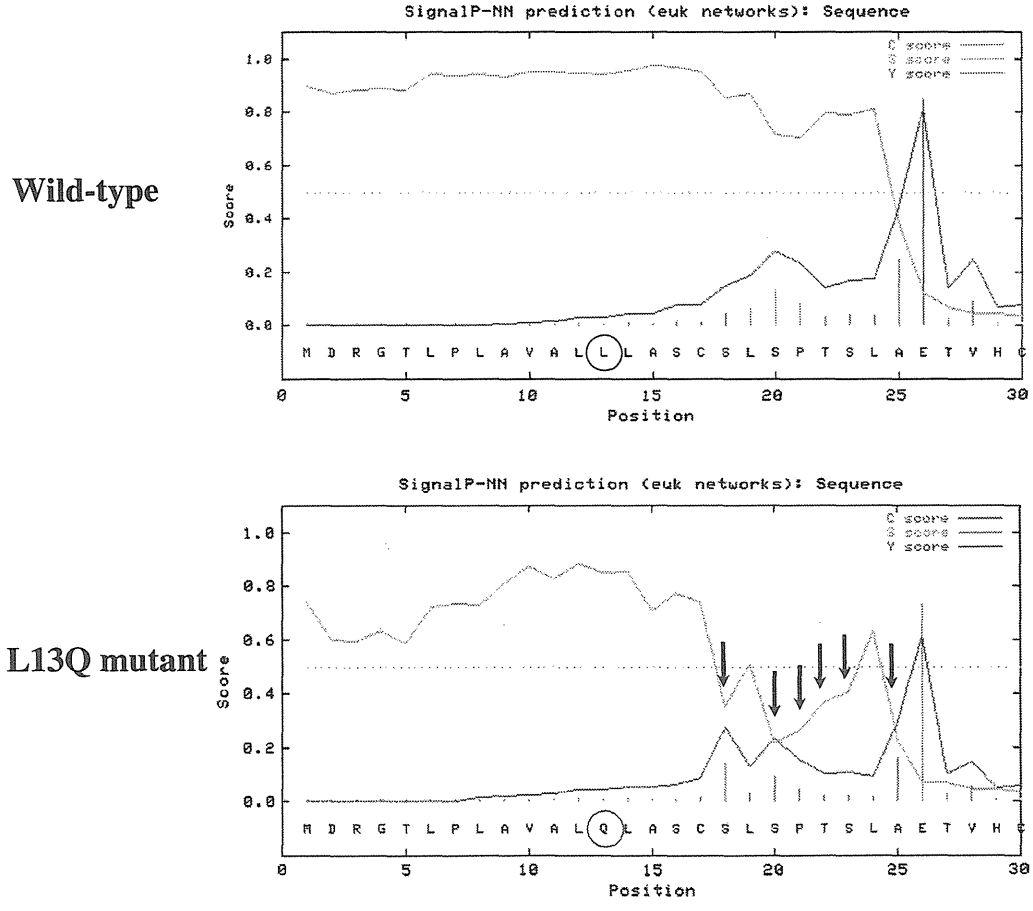


**Fig. 7. SignalP-NN analysis of endoglin signal sequences in wild-type and L13Q mutant.** N-terminal regions of the wild-type and L13Q mutant endoglins (black and red circles indicate wild-type 13Leu and mutant 13Gln, respectively) were analyzed with the SignalP-NN program (ver. 3.0). Attainment of signal peptide prediction (s-), cleavage site prediction (c-) and derived cleavage site prediction (y-) scores >50% cutoff values indicate proper signal peptide function and cleavage, whereas values below the cutoff indicate compromised function. A highly significant probability score of wild-type endoglin was obtained and the position of a signal cleavage site was predicted between amino acids 25Ala and 26Glu. However, SignalP-NN predictions for the signal peptide of the L13Q mutant showed that s-scores fell below the 50% cutoff after 18Ser except 19Leu and 24Leu (black arrows).

endoglin and perhaps stabilized the L13Q mutant. Further study is needed to clarify this phenomenon, but it might be due to the effect of glycosylation interference on the function of quality control system molecules themselves in the protein biosynthesis.

Endoglin is a co-receptor for the TGF-β receptor complex, modulating ALK1/ALK5 signaling and Smad transduction. We evaluated Smad3 phosphorylation induced by TGF-β in pL-ENG$^{L13Q}$-transfected EAhy926 cells, but any differences from the original and pL-ENG$^{WT}$-transfected EAhy926 cells were observed. These results suggested that the endogenous normal endoglin in EAhy926 cells would function sufficiently for TGF-β signaling Smad3 phosphorylation, and that the L13Q mutation in endoglin would not have a dominant negative effect on TGF-β signaling, which is a consistent result with the previous endoglin mutant study [38].

Appropriate targeting of proteins to subcellular compartments is an essential process in all living cells. Membrane proteins, such as endoglin, usually contain an amino-terminal signal peptide, which is recognized by the signal recognition particle (SRP) complex [39]. A universally conserved component of SRP binds to signal peptides, in which the total hydrophobicity of the h-region is a determinant for recognition [40]. The substitution of 13Leu with Gln in the center of the h-region of the endoglin signal peptide, which replaces a hydrophobic amino acid with a hydrophilic polar residue, would reduce hydrophobicity. Although we have no direct evidence, it might be possible that the mutated signal peptide of the L13Q endoglin would be impaired in the recognition by SRP.

Insight into whether particular amino acids in a signal sequence are consistent with signal peptide function can be gained with the SignalP-NN program [41]. The analysis of putative signal sequences in this way yields an s-score, which reports the signal peptide prediction for every single amino acid position with high s-cores indicating that the particular amino acid is part of a functioning signal peptide. SignalP-NN prediction for signal peptide of the wild-type endoglin showed that the s-score of L13Q mutant fell below the 50% cutoff after 18Ser except for 19Leu and 24Leu, suggesting that substitution of the hydrophobic 13Leu for a hydrophilic Gln might cause the collapse of its hydrophobic core and spoil its signal peptide function (Fig. 7). On the other hand, the mutation seemed to have no influence on the site of cleavage of the signal peptide according to c-scores and y-scores. Predictions of signal peptide function and cleavage sites suggested that the L13Q mutation would not affect the net charge, but it might be possible that the mutation would disturb the secondary structure of the signal peptide as a result of its abnormal -helix (h region), leading to poor recognition by SRP and failed insertion into the ER membrane. A comparison of endoglin sequences across species revealed that 13Leu was highly conserved attesting to its importance (Fig. 6).

In the present study, we identified a novel missense mutation in *ENG* (c.38 T > A, p.Leu13Gln), located in the hydrophobic core of the endoglin signal peptide. We also demonstrated disturbed cell-surface expression of the recombinant L13Q endoglin, which could lead to endoglin haploinsufficiency for HHT phenotype of the patient. In conclusion, this is the first report that the L13Q substitution of endoglin would be a causative mutation for HHT due to impaired co-translational processing of the protein.

## Conflict of interest statement

The authors have no coflicts of interest.

## Acknowledgements

We would like to thank Dr. Miyoko Matsushima and Dr. Tsutomu Kawabe for technical advice on flow cytometer management, and also Dr. Cora-Jean S. Edgell for the gift of EAhy926 cells. This study was partly supported by Grants-in-aid from the Ministry of Education, Culture, Sports, Science and Technology (22590524), and from the Ministry of Health and Welfare (Health Sciences Research Grant, Research on Specific Disease), Japan.

## Appendix A. Supplementary data

Supplementary data to this article can be found online at doi:10.1016/j.thromres.2011.12.030.

## References

[1] Guttmacher AE, Marchuk DA, White RI. Hereditary hemorrhagic telangiectasia. N Engl J Med 1995;333:918–24.
[2] Plauchu H, de Chadarévian JP, Bideau A, Robert JM. Age-related clinical profile of hereditary hemorrhagic telangiectasia in an epidemiologically recruited population. Am J Med Genet 1989;32:291–7.
[3] Berg J, Porteous M, Reinhardt D, et al. Hereditary haemorrhagic telangiectasia: a questionnaire based study to delineate the different phenotypes caused by endoglin and ALK1 mutations. J Med Genet 2003;40:585–90.
[4] Shovlin CL. Molecular defects in rare bleeding disorders: hereditary haemorrhagic telangiectasia. Thromb Haemost 1997;78:145–50.
[5] Fernández-L A, Sanz-Rodriguez F, Blanco FJ, Bernabéu C, Botella LM. Hereditary hemorrhagic telangiectasia, a vascular dysplasia affecting the TGF-beta signaling pathway. Clin Med Res 2006;4:66–78.
[6] Shovlin CL, Sulaiman NL, Govani FS, Jackson JE, Begbie ME. Elevated factor VIII in hereditary haemorrhagic telangiectasia (HHT): association with venous thromboembolism. Thromb Haemost 2007;98:1031–9.
[7] McDonald MT, Papenberg KA, Ghosh S, et al. A disease locus for hereditary haemorrhagic telangiectasia maps to chromosome 9q33-34. Nat Genet 1994;6:197–204.
[8] Shovlin CL, Hughes JM, Tuddenham EG, et al. A gene for hereditary haemorrhagic telangiectasia maps to chromosome 9q3. Nat Genet 1994;6:205–9.
[9] McAllister KA, Grogg KM, Johnson DW, et al. Endoglin, a TGF-beta binding protein of endothelial cells, is the gene for hereditary haemorrhagic telangiectasia type 1. Nat Genet 1994;8:345–51.
[10] Vincent P, Plauchu H, Hazan J, Fauré S, Weissenbach J, Godet J. A third locus for hereditary haemorrhagic telangiectasia maps to chromosome 12q. Hum Mol Genet 1995;4:945–9.
[11] Johnson DW, Berg JN, Gallione CJ, et al. A second locus for hereditary hemorrhagic telangiectasia maps to chromosome 12. Genome Res 1995;5:21–8.
[12] Johnson DW, Berg JN, Baldwin MA, et al. Mutations in the activin receptor-like kinase 1 gene in hereditary haemorrhagic telangiectasia type 2. Nat Genet 1996;13:189–95.
[13] López-Novoa JM, Bernabeu C. The physiological role of endoglin in the cardiovascular system. Am J Physiol Heart Circ Physiol 2010;299:H959–74.
[14] Shovlin CL, Hughes JM, Scott J, Seidman CE, Seidman JG. Characterization of endoglin and identification of novel mutations in hereditary hemorrhagic telangiectasia. Am J Hum Genet 1997;61:68–79.
[15] Lux A, Attisano L, Marchuk DA. Assignment of transforming growth factor beta1 and beta3 and a third new ligand to the type I receptor ALK-1. J Biol Chem 1999;274:9984–92.
[16] Gougos A, Letarte M. Identification of a human endothelial cell antigen with monoclonal antibody 44G4 produced against a pre-B leukemic cell line. J Immunol 1988;141:1925–33.
[17] Attisano L, Cárcamo J, Ventura F, Weis FM, Massagué J, Wrana JL. Identification of human activin and TGF beta type I receptors that form heteromeric kinase complexes with type II receptors. Cell 1993;75:671–80.
[18] Attisano L, Wrana JL. Signal transduction by the TGF-beta superfamily. Science 2002;296:1646–7.
[19] Derynck R, Zhang YE. Smad-dependent and Smad-independent pathways in TGF-beta family signalling. Nature 2003;425:577–84.
[20] Lebrin F, Goumans MJ, Jonker L, et al. Endoglin promotes endothelial cell proliferation and TGF-beta/ALK1 signal transduction. EMBO J 2004;23:4018–28.
[21] Suzuki A, Sanda N, Miyawaki Y, et al. Down-regulation of PROS1 gene expression by 17beta-estradiol via estrogen receptor alpha (ERalpha)-Sp1 interaction recruiting receptor-interacting protein 140 and the corepressor-HDAC3 complex. J Biol Chem 2010;285:13444–53.
[22] Goumans MJ, Valdimarsdottir G, Itoh S, Rosendahl A, Sideras P, ten Dijke P. Balancing the activation state of the endothelium via two distinct TGF-beta type I receptors. EMBO J 2002;21:1743–53.
[23] Goumans MJ, Valdimarsdottir G, Itoh S, et al. Activin receptor-like kinase (ALK)1 is an antagonistic mediator of lateral TGFbeta/ALK5 signaling. Mol Cell 2003;12:817–28.
[24] Lastres P, Letamendía A, Zhang H, et al. Endoglin modulates cellular responses to TGF-beta 1. J Cell Biol 1996;133:1109–21.
[25] Bellón T, Corbí A, Lastres P, et al. Identification and expression of two forms of the human transforming growth factor-beta-binding protein endoglin with distinct cytoplasmic regions. Eur J Immunol 1993;23:2340–5.
[26] Abdalla SA, Letarte M. Hereditary haemorrhagic telangiectasia: current views on genetics and mechanisms of disease. J Med Genet 2006;43:97–110.
[27] Jerkic M, Rodríguez-Barbero A, Prieto M, et al. Reduced angiogenic responses in adult Endoglin heterozygous mice. Cardiovasc Res 2006;69:845–54.

[28] Gallione CJ, Klaus DJ, Yeh EY, et al. Mutation and expression analysis of the endoglin gene in hereditary hemorrhagic telangiectasia reveals null alleles. Hum Mutat 1998;11:286–94.
[29] Letteboer TG, Zewald RA, Kamping EJ, et al. Hereditary hemorrhagic telangiectasia: ENG and ALK-1 mutations in Dutch patients. Hum Genet 2005;116:8–16.
[30] Bourdeau A, Faughnan ME, Letarte M. Endoglin-deficient mice, a unique model to study hereditary hemorrhagic telangiectasia. Trends Cardiovasc Med 2000;10:279–85.
[31] Lesca G, Plauchu H, Coulet F, et al. Molecular screening of ALK1/ACVRL1 and ENG genes in hereditary hemorrhagic telangiectasia in France. Hum Mutat 2004;23:289–99.
[32] Bossler AD, Richards J, George C, Godmilow L, Ganguly A. Novel mutations in ENG and ACVRL1 identified in a series of 200 individuals undergoing clinical genetic testing for hereditary hemorrhagic telangiectasia (HHT): correlation of genotype with phenotype. Hum Mutat 2006;27:667–75.
[33] Martoglio B, Dobberstein B. Signal sequences: more than just greasy peptides. Trends Cell Biol 1998;8:410–5.
[34] von Heijne G. The signal peptide. J Membr Biol 1990;115:195–201.
[35] Pidasheva S, Canaff L, Simonds WF, Marx SJ, Hendy GN. Impaired cotranslational processing of the calcium-sensing receptor due to signal peptide missense mutations in familial hypocalciuric hypercalcemia. Hum Mol Genet 2005;14:1679–90.
[36] Paquet ME, Pece-Barbara N, Vera S, et al. Analysis of several endoglin mutants reveals no endogenous mature or secreted protein capable of interfering with normal endoglin function. Hum Mol Genet 2001;10:1347–57.
[37] Lux A, Gallione CJ, Marchuk DA. Expression analysis of endoglin missense and truncation mutations: insights into protein structure and disease mechanisms. Hum Mol Genet 2000;9:745–55.
[38] Pece N, Vera S, Cymerman U, White RI, Wrana JL, Letarte M. Mutant endoglin in hereditary hemorrhagic telangiectasia type 1 is transiently expressed intracellularly and is not a dominant negative. J Clin Invest 1997;100:2568–79.
[39] Janda CY, Li J, Oubridge C, Hernández H, Robinson CV, Nagai K. Recognition of a signal peptide by the signal recognition particle. Nature 2010;465:507–10.
[40] Hatsuzawa K, Tagaya M, Mizushima S. The hydrophobic region of signal peptides is a determinant for SRP recognition and protein translocation across the ER membrane. J Biochem 1997;121:270–7.
[41] Bendtsen JD, Nielsen H, von Heijne G, Brunak S. Improved prediction of signal peptides: SignalP 3.0. J Mol Biol 2004;340:783–95.

BRIEF REPORT

# Thrombosis from a Prothrombin Mutation Conveying Antithrombin Resistance

Yuhri Miyawaki, M.Sc., Atsuo Suzuki, M.Sc., Junko Fujita, B.Sc., Asuka Maki, B.Sc., Eriko Okuyama, B.Sc., Moe Murata, B.Sc., Akira Takagi, Ph.D., Takashi Murate, M.D., Ph.D., Shinji Kunishima, Ph.D., Michio Sakai, M.D., Kohji Okamoto, M.D., Ph.D., Tadashi Matsushita, M.D., Ph.D., Tomoki Naoe, M.D., Ph.D., Hidehiko Saito, M.D., Ph.D., and Tetsuhito Kojima, M.D., Ph.D.

From the Departments of Pathophysiological Laboratory Sciences (Y.M., A.S., J.F., A.M., E.O., M.M., A.T., T. Murate, T.K.) and Hematology–Oncology (T.N.), Nagoya University Graduate School of Medicine, the Department of Medical Technology, Nagoya University School of Health Sciences (A.T., T. Murate, T.K.), the Department of Advanced Diagnosis, Clinical Research Center (S.K.), National Hospital Organization, Nagoya Medical Center (S.K., H.S.), and the Department of Transfusion Medicine, Nagoya University Hospital (T. Matsushita), Nagoya; and the Departments of Pediatrics (M.S.) and Surgery 1 (K.O.), University of Occupational and Environmental Health, Kita-kyushu — all in Japan. Address reprint requests to Dr. Kojima at the Department of Medical Technology, Nagoya University School of Health Sciences, 1-1-20 Daiko-Minami, Higashi-ku, Nagoya 461-8673, Japan, or at kojima@met.nagoya-u.ac.jp.

N Engl J Med 2012;366:2390-6.


## SUMMARY

We identified a novel mechanism of hereditary thrombosis associated with antithrombin resistance, with a substitution of arginine for leucine at position 596 (p.Arg596Leu) in the gene encoding prothrombin (called prothrombin Yukuhashi). The mutant prothrombin had moderately lower activity than wild-type prothrombin in clotting assays, but the formation of thrombin–antithrombin complex was substantially impaired. A thrombin-generation assay revealed that the peak activity of the mutant prothrombin was fairly low, but its inactivation was extremely slow in reconstituted plasma. The Leu596 substitution caused a gain-of-function mutation in the prothrombin gene, resulting in resistance to antithrombin and susceptibility to thrombosis.

PATIENTS WITH HEREDITARY THROMBOPHILIA OFTEN PRESENT WITH UNusual clinical episodes of venous thrombosis at a young age and recurrence in atypical vessels, often with a family history of the condition.[1] Genetic studies of hereditary thrombophilia have revealed two types of genetic defects: loss-of-function mutations in the natural anticoagulants antithrombin, protein C, and protein S, along with gain-of-function mutations in procoagulant factors V (factor V Leiden) and II (prothrombin G20210A).[2] To date, numerous genetic defects have been found in families with hereditary thrombophilia, but there may be many undiscovered causative mutations.[3] Here, we describe a case of hereditary thrombosis induced by a novel mechanism of antithrombin resistance, a gain-of-function mutation in the gene encoding the clotting factor prothrombin (prothrombin Yukuhashi).

## CASE REPORT

The proband was a 17-year-old Japanese girl who had a first episode of deep-vein thrombosis at the age of 11 years and had since been treated with warfarin. Her family originated in Yukuhashi in the northern part of the Kyushu islands. At least nine of her family members had had one or more episodes of deep-vein thrombosis (Fig. 1A), including two with pulmonary embolism and three who died from thrombosis. Five family members, including the proband, had had juvenile thrombosis, with two reporting episodes during early childhood. Previous studies did not identify any known causes of hereditary thrombophilia in this family.[4]

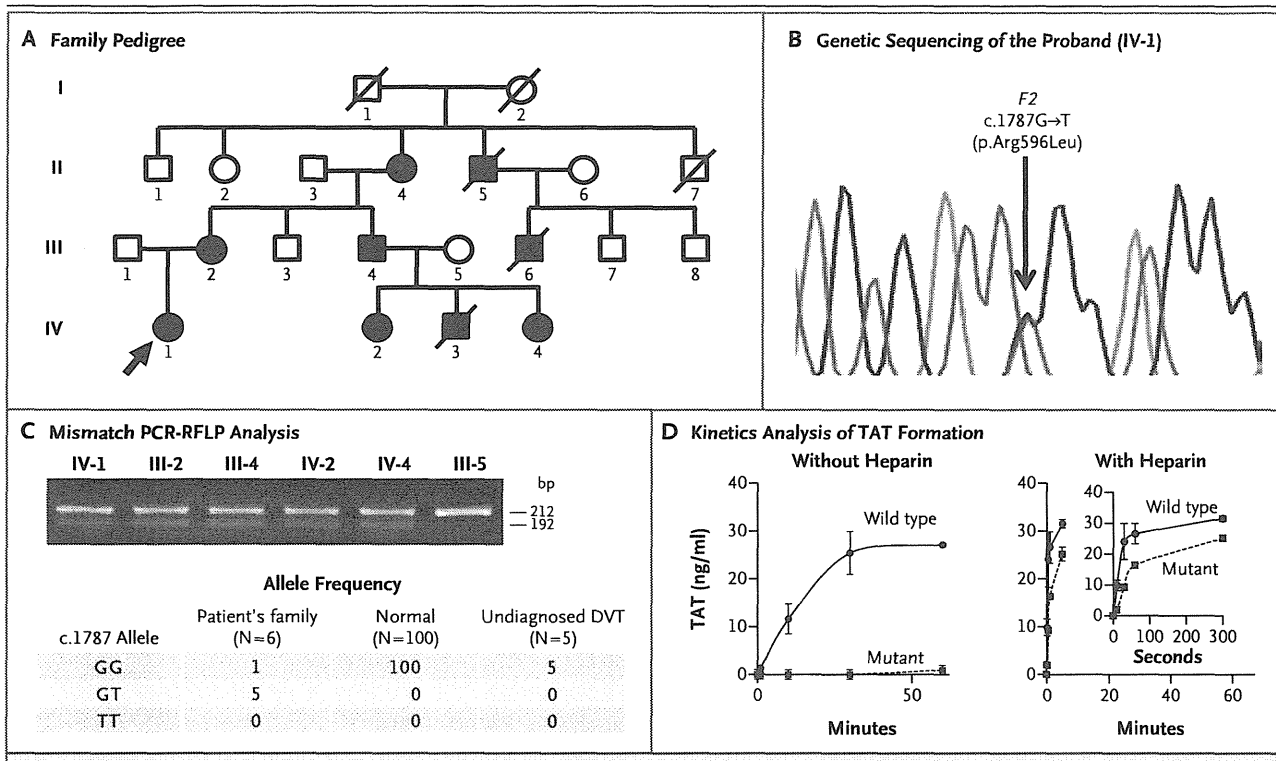


Figure 1. **Prothrombin Genotype of a Family with Hereditary Thrombophilia.**

Panel A shows the family pedigree. The proband (IV-1) is indicated by an arrow. Solid symbols represent affected family members, open symbols unaffected family members, and slashed symbols deceased family members. Circles represent female family members, and squares male family members. Panel B shows the sequence of the prothrombin gene around the site of the mutation in exon 14. A G→T transversion at nucleotide 1787 of the coding sequence (c.1787G→T) has occurred in the gene encoding the clotting factor prothrombin Yukuhashi, resulting in an amino acid substitution of leucine for arginine at position 596 (p.Arg596Leu). The proband is heterozygous for the mutation (arrow). Panel C shows a restriction-fragment–length polymorphism (RFLP) analysis of the mismatch polymerase-chain-reaction (PCR) product of exon 14 of the prothrombin gene digested by PstI endonuclease. The wild-type prothrombin gene has an undigested fragment of 212 bp. The mutation in the prothrombin Yukuhashi gene creates a PstI site, resulting in a digestion fragment of 192 bp. The table shows allele frequencies at c.1787 of the prothrombin gene in 6 family members, in 100 Japanese persons with a normal phenotype, and in 5 persons with previously undiagnosed deep-vein thrombosis (DVT). Panel D shows the kinetics analysis of thrombin–antithrombin complex (TAT) formation of recombinant wild-type and p.Arg596Leu mutant prothrombins, in the presence and absence of heparin. TAT levels were measured with the use of an enzyme-linked immunosorbent assay and various incubation times for antithrombin and recombinant thrombins; the latter are forms of recombinant prothrombins activated by factor Xa.

## METHODS

### DNA ANALYSIS

We amplified all 14 exons, including the exon–intron boundaries and the 3′ untranslated region, of the prothrombin gene by means of polymerase chain reaction (PCR), using gene-specific primers (see Table S1 in the Supplementary Appendix, available with the full text of this article at NEJM .org). The amplicons were sequenced as described previously.[5] To detect the mutation, we performed PCR–restriction-fragment–length polymorphism (RFLP) analysis, using a mismatched lower primer (5′-TGTAGAAGCCATATTTCCCcTgC-3′, with base substitutions at c and g) and introducing a PstI site into the amplicon from a mutant allele. Genomic DNA was isolated from peripheral leukocytes by phenol extraction.[6]

### RECOMBINANT PROTHROMBINS

We used a PCR assay to prepare full-length human prothrombin complementary DNA (cDNA) obtained from a human liver cDNA library (Clontech) and cloned this into pcDNA™3.1(+) (Invitrogen) to obtain a wild-type human prothrombin expression vector. Subsequently, we prepared a mutant prothrombin expression vector by means of overlap extension PCR,[7] using two primers: 5′-TGAAGGCTGTGACCtGGATGGGAAA-3′ (sense primer with a base substitution at t) and

5′-TTTCCCATCCaGGTCACAGCCTTCA-3′ (antisense primer with a base substitution at a).

We transfected human embryonic kidney cells (HEK293) with the prothrombin expression vectors using the calcium phosphate method.[8] We established stable transformants by selection with G418 and determined which of these had high levels of prothrombin expression by means of a dot-blot immunoassay. Conditioned media of stable transformants expressing recombinant prothrombins in serum-free medium containing vitamin K were collected, concentrated, and stored at −80°C until use. We determined the antigen levels of the prothrombins using an enzyme-linked immunosorbent assay (ELISA, Enzyme Research Laboratories).

### FUNCTIONAL ASSAYS OF RECOMBINANT PROTHROMBINS

We performed three tests of prothrombin activity: a one-stage clotting assay, a two-stage clotting assay, and a chromogenic assay that uses S-2238 (a thrombin substrate that generates color at the time of cleavage). In the latter two assays, we used *Oxyuranus scutellatus* venom (Sigma Aldrich) as a factor Xa–like enzyme. To examine the functions of the recombinant prothrombins in plasma, we prepared reconstituted plasma by mixing prothrombin-deficient plasma (prothrombin activity, <1%; Mitsubishi Chemical Medience) with the recombinant prothrombins on the assumption that the prothrombin concentration was 100 μg per milliliter in normal plasma (100%).[9] The proband's plasma was not suitable for evaluation because of warfarin treatment.

### FORMATION OF THROMBIN–ANTITHROMBIN COMPLEX

To evaluate the ability of the wild-type and mutant recombinant prothrombins to form complexes with antithrombin, we converted the recombinant prothrombins to thrombins, using bovine factors Xa (Haematologic Technologies) and Va (Thermo Scientific), cephalin (Roche Diagnostica Stago), and calcium chloride. We then incubated the thrombins with human antithrombin (Mitsubishi Tanabe Pharma), with or without unfractionated heparin (Mochida Pharmaceutical), at 37°C for various time periods. The reactions were stopped with PPACK (D-phenylalanyl-L-prolyl-L-arginine chloromethyl ketone) (Calbiochem), and thrombin–antithrombin complex formation was measured with the use of the AssayMax Human TAT Complexes ELISA kit (Assaypro).

### THROMBIN-GENERATION ASSAY

We prepared wild-type, mutant, and heterozygous-mutant reconstituted plasma by mixing prothrombin-deficient plasma with the recombinant prothrombins, at a final prothrombin concentration of 100%, and by mixing antithrombin-depleted plasma (Affinity Biologicals) with human antithrombin, at a final antithrombin concentration of 50%. We used normal pooled plasma as a control. The thrombin-generation assay was performed by means of calibrated automated thrombography (CAT, Thrombinoscope BV), in accordance with the manufacturer's instructions. We monitored the reactions for 2 hours, using Fluoroscan Ascent FL (Thermo LabSystems), set at an excitation wavelength of 390 nm and an emission wavelength of 460 nm, and Thrombinoscope software (Thrombinoscope BV).

### STUDY OVERSIGHT

The study was approved by the ethics committee at the Nagoya University School of Medicine. Written informed consent was obtained from all study participants.

## RESULTS

### DNA ANALYSIS

Genomic DNA analysis of the proband revealed that she was heterozygous for a novel missense mutation in the prothrombin gene (c.1787G→T, p.Arg596Leu) (Fig. 1B). The nucleotide and protein numbering system is based on the nomenclature recommended by the Human Genome Variation Society.[10] The same mutation was detected in her mother and in three other family members with deep-vein thrombosis but not in an asymptomatic family member. On mismatch PCR-RFLP analysis, the amplicon that was treated with PstI displayed a 192-bp band (mutant allele) and a 212-bp band (normal allele). We confirmed the heterozygosity of this mutation in the proband, her mother, and three other family members with deep-vein thrombosis but not in an asymptomatic family member (Fig. 1C). We did not detect the mutation in samples obtained from 100 Japanese persons with a normal phenotype and in 5 persons with undiagnosed thrombosis before this testing.

### RECOMBINANT PROTHROMBINS

We established stable transformants of HEK293 cells expressing the wild-type and mutant prothrombins. To evaluate γ-carboxylation of the recombinant prothrombins, we used ELISA to measure prothrombin levels in the culture medium after barium sulfate absorption. We found that both the wild-type and mutant prothrombins were completely absorbed, suggesting that appropriate γ-carboxylation occurred in both preparations (data not shown).

### FUNCTIONAL ASSAYS OF RECOMBINANT PROTHROMBINS

We performed three assessments of recombinant prothrombin activity: one-stage clotting, two-stage clotting, and chromogenic assays (Table 1). Reconstituted plasma was used in all tests. Values for the wild-type recombinant prothrombin were approximately 100% in all assays. The mutant prothrombin activity in the one-stage assay was lower than that in the two-stage assay. The mutant prothrombin activity in the chromogenic assay was higher than that in the two-stage assay.

### FORMATION OF THROMBIN–ANTITHROMBIN COMPLEX

We used ELISA to determine whether there was a difference between the wild-type and mutant prothrombins in forming thrombin–antithrombin complexes. The recombinant prothrombins that were activated by factor Xa were incubated with antithrombin, and thrombin–antithrombin complex formation was determined by means of ELISA. In the absence of heparin, thrombin–antithrombin complex formation by the wild-type prothrombin increased in a time-dependent manner. However, thrombin–antithrombin complex formation by the mutant prothrombin was almost negligible for the first 30 minutes (Fig. 1D). In the presence of heparin, thrombin–antithrombin complex formation was greatly increased in both samples but remained substantially impaired in the mutant sample.

### THROMBIN-GENERATION ASSAY

A thrombin-generation assay was performed to evaluate the effect of the mutation on thrombin generation in plasma (Fig. 2). The values for wild-type reconstituted plasma were similar to those for normal plasma, but the mutant plasma showed a decreased maximum concentration of thrombin (peak), an extension of the total duration of thrombin-generation activity (start tail), and increased thrombin activity, which was assessed as the area under the curve for endogenous thrombin potential. The heterozygous-mutant plasma, mimicking the proband's plasma, showed intermediate values. The 50% antithrombin plasma, mimicking the antithrombin-deficient plasma, showed similar changes (except for a decreased peak), which were canceled by the addition of human antithrombin at a final concentration of 150%. These data indicate that the thrombin activity derived from the mutant prothrombin was lower than that derived from the wild-type prothrombin, but its inactivation was exceedingly slow, resulting in a prolonged procoagulant state in the proband's plasma.

Table 1. **Procoagulant and Amidolytic Activities of the Recombinant Prothrombins.***

| Prothrombin | Antigen† | Activity‡ | | |
|---|---|---|---|---|
| | | One-Stage Clotting Assay | Two-Stage Clotting Assay | Chromogenic Assay |
| | | *percent* | | |
| Wild-type | 112 | 91 | 109 | 88 |
| Mutant | 118 | 15 | 32 | 66 |

* The values were measured in reconstituted prothrombin-deficient plasma. The value of normal plasma was assigned as 100%.

† The values for prothrombin antigens were determined by means of enzyme-linked immunosorbent assay.

‡ The prothrombin activities were determined by three methods: the classic one-stage clotting assay, in which thromboplastin is used; the two-stage clotting assay, in which *Oxyuranus scutellatus* venom (Ox) is used as a factor Xa–like enzyme and fibrinogen from pooled normal plasma is used as a substrate; and the chromogenic assay, in which Ox venom is used as an activator and S-2238 as a substrate.

## DISCUSSION

Numerous gene mutations in various molecules have been found in members of families with inherited thrombophilia, but many mutations remain unidentified.[3] The G20210A mutation in the prothrombin gene is associated with a mild risk of thrombosis in the white population, but many other prothrombin gene mutations lead to bleeding tendencies, such as prothrombin deficiencies, dysprothrombinemia, and hypoprothrombinemia.[11-13] A genomewide analysis to detect genes that are associated with a susceptibility to thrombosis also identified a prothrombin gene mutation, but the detailed molecular mechanism for

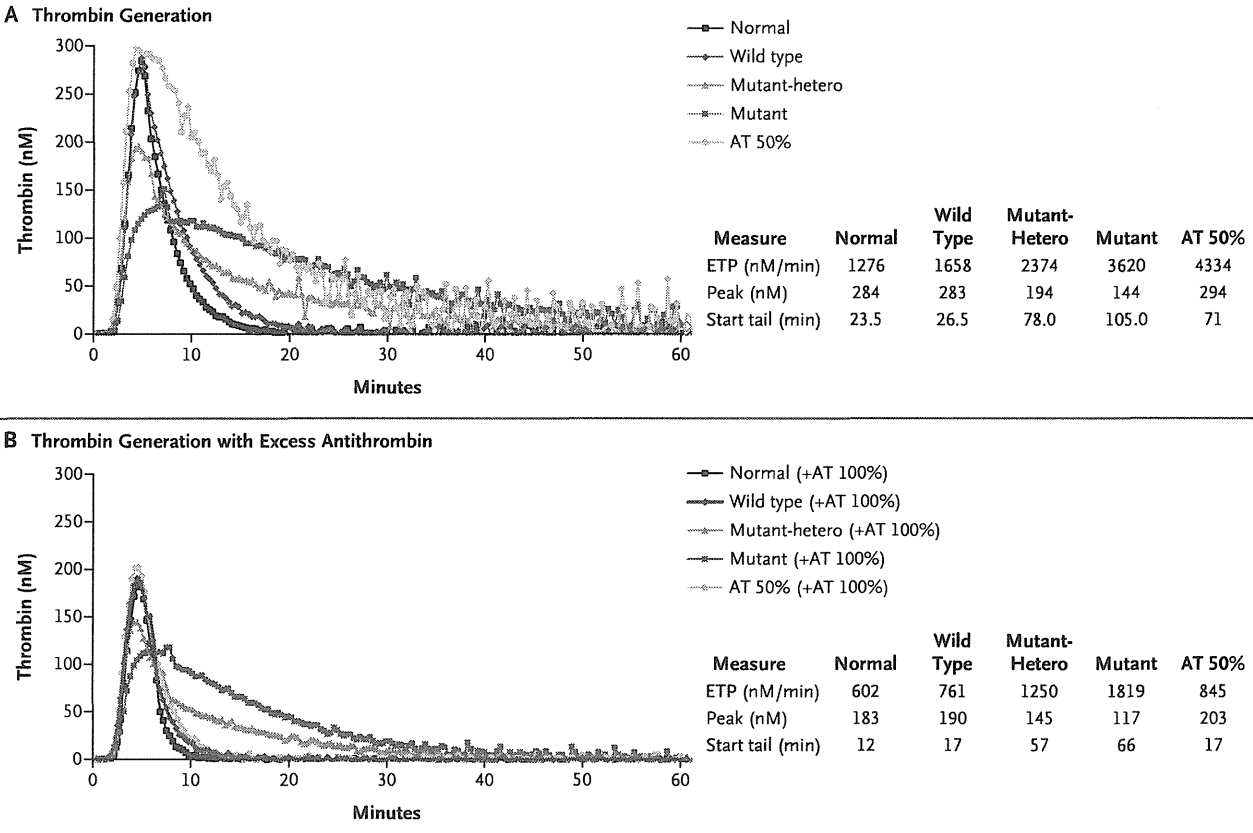


| Measure | Normal | Wild Type | Mutant-Hetero | Mutant | AT 50% |
|---|---|---|---|---|---|
| ETP (nM/min) | 1276 | 1658 | 2374 | 3620 | 4334 |
| Peak (nM) | 284 | 283 | 194 | 144 | 294 |
| Start tail (min) | 23.5 | 26.5 | 78.0 | 105.0 | 71 |

| Measure | Normal | Wild Type | Mutant-Hetero | Mutant | AT 50% |
|---|---|---|---|---|---|
| ETP (nM/min) | 602 | 761 | 1250 | 1819 | 845 |
| Peak (nM) | 183 | 190 | 145 | 117 | 203 |
| Start tail (min) | 12 | 17 | 57 | 66 | 17 |

**Figure 2. Thrombin-Generation Assays with and without Excess Antithrombin.**

Panel A shows the results of a thrombin-generation assay of normal plasma as well as reconstituted plasma samples, with recombinant prothrombins in prothrombin-deficient plasma and of human antithrombin (AT 50%) in antithrombin-depleted plasma. The heterozygous-mutant (mutant-hetero) plasma contained 50% each of wild-type and mutant prothrombin. The table at the right shows the total amount of thrombin activity, which was assessed as the area under the curve for endogenous thrombin potential (ETP), the maximum concentration of thrombin (peak), and the total duration of thrombin-generation activity (start tail). Panel B shows the results of a thrombin-generation assay of the respective plasma samples after the addition of excess antithrombin.

inherited thrombophilia remains unknown.[14] In this study, we investigated possible causative genetic defects in samples obtained from a large Japanese family with inherited thrombophilia. We found a novel missense mutation in the prothrombin gene (p.Arg596Leu) that resulted in a variant prothrombin (prothrombin Yukuhashi). The mutation cosegregated with deep-vein thrombosis in this family, indicating that it could be a cause of hereditary thrombophilia.

Thrombin, which is an active form of prothrombin, is an allosteric enzyme controlled by the binding of sodium.[15,16] Sodium-bound thrombin (known as the fast form) is optimized for procoagulation because of its increased substrate specificity for fibrinogen, whereas sodium-free thrombin (known as the slow form) is an anticoagulant because of its increased specificity for cleaving protein C. The mutation occurred at residue Arg596 (Arg221a in the chymotrypsinogen numbering system[17]) within the sodium-binding region of thrombin and was expected to have an effect on sodium binding. The mutation is also located at one of the antithrombin-binding sites where thrombin is inactivated by antithrombin with heparin.[18] Two exosites on thrombin, the γ-loop and the sodium-binding region, are critical for stabilizing a thrombin–antithrombin complex[18] (Fig. S1A in the Supplementary Appendix). Two hydrogens of the Arg596 side chains of thrombin form hydrogen bonds with oxygen of the Asn265 side chain of antithrombin (Fig. S1B in the Supplementary Appendix). Therefore, we propose two hypotheses: first, that the procoagu-

lant activity of the mutant prothrombin is somewhat impaired; and second, that complex formation involving the mutant thrombin and antithrombin is impaired, resulting in prolonged residual thrombin activity.

To test the first hypothesis, we examined the activation and procoagulant functions of the recombinant prothrombins. We prepared reconstituted plasma by mixing prothrombin-deficient plasma with the recombinant prothrombins, since the proband's plasma was not suitable for evaluation because of warfarin treatment. We observed that the mutant and wild-type prothrombins were fully converted to thrombins in a similar manner by prothrombinase within 5 minutes (Fig. S2 in the Supplementary Appendix). However, conversion of the mutant prothrombin to thrombin appeared to be a few seconds slower than that of the wild-type thrombin in the clotting assays. In addition, the mutant thrombin probably had a lower catalytic activity for fibrinogen than did the wild-type thrombin, which may have been the result of structural disruption of the sodium-binding region by the Leu596 substitution for Arg. In a previous study of alanine-scanning mutagenesis, thrombin with an Ala596 mutation showed a reduction by a factor of 5 in sodium-binding affinity, and its procoagulant activity was similar to that of the slow form of thrombin.[19] Similar mechanisms of structural disruption in the Leu596 mutant thrombin may have resulted in lower catalytic activity for fibrinogen.

To test the second hypothesis — that the mutant thrombin would be defective in terms of its interaction with antithrombin — we examined thrombin–antithrombin complex formation using ELISA. The mutant thrombin sample had extremely low levels of thrombin–antithrombin complex formation. This suggests that the disruption of the sodium-binding region, which resulted in the loss of two hydrogen bonds between Arg596 of thrombin and Asn265 of antithrombin, may be critical for the formation of the thrombin–antithrombin complex. These findings indicate that prothrombin Yukuhashi can be characterized as a dysprothrombin that is highly resistant to inhibition by antithrombin.

We next performed a thrombin-generation assay to determine the potential procoagulant activity of the recombinant prothrombins in plasma. A thrombin-generation assay is a comprehensive coagulation-function test that allows evaluation not only of the initial phase of thrombin generation but also of the late phase of its inactivation. Data from this assay again suggested that the mutant prothrombin had low procoagulant activity but was highly resistant to antithrombin. Thus, its active form, the mutant thrombin, would not be inactivated by antithrombin and would continue to facilitate blood coagulation, despite its low activity level.

In conclusion, we identified a novel mechanism of hereditary thrombosis in a Japanese family, in which antithrombin resistance was associated with a missense mutation in the prothrombin gene (p.Arg596Leu). This mutation results in slightly impaired but adequate procoagulant function of the mutant prothrombin but considerably impaired inhibition of the mutant thrombin by antithrombin. The antithrombin-resistant thrombin may have prolonged procoagulant activity in vivo, conferring a susceptibility to thrombosis.

Supported in part by grants from the Japanese Ministry of Education, Culture, Sports, Science, and Technology; the Japanese Ministry of Health, Labor and Welfare; and the Senshin Medical Research Foundation.

Disclosure forms provided by the authors are available with the full text of this article at NEJM.org.

We thank C. Wakamatsu for providing technical assistance, and Enago for translation services.

REFERENCES

1. De Stefano V, Finazzi G, Mannucci P. Inherited thrombophilia: pathogenesis, clinical syndromes, and management. Blood 1996;87:3531-44.
2. Rosendaal FR. Venous thrombosis: a multicausal disease. Lancet 1999;353:1167-73.
3. Khan S, Dickerman JD. Hereditary thrombophilia. Thromb J 2006;4:15.
4. Sakai M, Urano H, Iinuma A, Okamoto K, Ohsato K, Shirahata A. A family with multiple thrombosis including infancy occurrence. J UOEH 2001;23:297-305. (In Japanese.)
5. Okada H, Takagi A, Murate T, et al. Identification of protein S alpha gene mutations including four novel mutations in eight unrelated patients with protein S deficiency. Br J Haematol 2004;126:219-25.
6. Kojima T, Tanimoto M, Kamiya T, et al. Possible absence of common polymorphisms in coagulation factor IX gene in Japanese subjects. Blood 1987;69:349-52.
7. Suzuki A, Nakashima D, Miyawaki Y, et al. A novel ENG mutation causing impaired co-translational processing of endoglin associated with hereditary hemorrhagic telangiectasia. Thromb Res 2012;129(5):e200-e208.
8. Suzuki A, Sanda N, Miyawaki Y, et al. Down-regulation of PROS1 gene expression by 17β-estradiol via estrogen receptor α (ERα)-Sp1 interaction recruiting receptor-interacting protein 140 and the corepressor-HDAC3 complex. J Biol Chem 2010;285:13444-53.

9. Lundblad RL, Kingdon HS, Mann KG. Thrombin. Methods Enzymol 1976;45:156-76.
10. den Dunnen JT, Antonarakis SE. Mutation nomenclature extensions and suggestions to describe complex mutations: a discussion. Hum Mutat 2000;15:7-12. [Erratum, Hum Mutat 2002;20:403.]
11. Akhavan S, Mannucci P, Lak M, et al. Identification and three-dimensional structural analysis of nine novel mutations in patients with prothrombin deficiency. Thromb Haemost 2000;84:989-97.
12. Lefkowitz JB, Weller A, Nuss R, Santiago-Borrero PJ, Brown DL, Ortiz IR. A common mutation, Arg457→Gln, links prothrombin deficiencies in the Puerto Rican population. J Thromb Haemost 2003;1:2381-8.
13. Poort SR, Rosendaal FR, Reitsma PH, Bertina RM. A common genetic variation in the 3′-untranslated region of the prothrombin gene is associated with elevated plasma prothrombin levels and an increase in venous thrombosis. Blood 1996;88:3698-703.
14. ten Kate M, He C, van Schouwenburg I, et al. A genome wide linkage scan for thrombosis susceptibility genes identifies a novel prothrombin mutation. Presented at the 22nd Congress of the International Society on Thrombosis and Haematosis, Boston, July 11–16, 2009. abstract.
15. Dang QD, Vindigni A, Di Cera E. An allosteric switch controls the procoagulant and anticoagulant activities of thrombin. Proc Natl Acad Sci U S A 1995;92:5977-81.
16. Pineda AO, Carrell CJ, Bush LA, et al. Molecular dissection of $Na^+$ binding to thrombin. J Biol Chem 2004;279:31842-53.
17. Bode W, Turk D, Karshikov A. The refined 1.9-Å X-ray crystal structure of d-Phe-Pro-Arg chloromethylketone-inhibited human $\alpha$-thrombin: structure analysis, overall structure, electrostatic properties, detailed active-site geometry, and structure-function relationships. Protein Sci 1992;1:426-71.
18. Li W, Johnson DJD, Esmon CT, Huntington JA. Structure of the antithrombin-thrombin-heparin ternary complex reveals the antithrombotic mechanism of heparin. Nat Struct Mol Biol 2004;11:857-62.
19. Dang QD, Guinto ER, Cera ED. Rational engineering of activity and specificity in a serine protease. Nat Biotechnol 1997;15:146-9.

*Journal of Thrombosis and Haemostasis*, **10**: 2099–2107 DOI: 10.1111/j.1538-7836.2012.04897.x

ORIGINAL ARTICLE

# A possible mechanism for Inv22-related *F8* large deletions in severe hemophilia A patients with high responding factor VIII inhibitors

J. FUJITA,* Y. MIYAWAKI,* A. SUZUKI,*† A. MAKI,* E. OKUYAMA,* M. MURATA,* A. TAKAGI,*‡ T. MURATE,*‡ N. SUZUKI,§ T. MATSUSHITA,¶ H. SAITO** and T. KOJIMA*‡

**Department of Pathophysiological Laboratory Sciences, Nagoya University Graduate School of Medicine, Nagoya; †Japan Society for the Promotion of Science, Tokyo; ‡Department of Medical Technology, Nagoya University School of Health Sciences, Nagoya; §Department of Clinical Laboratory, Nagoya University Hospital, Nagoya; ¶Department of Blood Transfusion Service, Nagoya University Hospital, Nagoya; and **National Hospital Organization Nagoya Medical Center, Nagoya, Japan*

**To cite this article:** Fujita J, Miyawaki Y, Suzuki A, Maki A, Okuyama E, Murata M, Takagi A, Murate T, Suzuki N, Matsushita T, Saito H, Kojima T. A possible mechanism for Inv22-related *F8* large deletions in severe hemophilia A patients with high responding factor VIII inhibitors. *J Thromb Haemost* 2012; **10**: 2099–107.

**Summary.** *Background:* Intron 22 inversion (Inv22) of the coagulation factor (F)VIII gene (*F8*) is a frequent cause of severe hemophilia A. In addition to Inv22, a variety of *F8* mutations (1492 unique mutations) causing hemophilia A have been reported, of which 171 involve deletions of over 50 bp (HAMSTeRs database; http://hadb.org.uk/). However, only 10% of these large deletions have been fully characterized at the nucleotide level. *Patients and methods:* We investigated gene abnormalities in three unrelated severe hemophilia A patients with high titer FVIII inhibitors. They had previously been shown to carry large deletions of the *F8*, but the precise gene abnormalities remain to be elucidated. *Results:* Inverse shifting-PCR (IS-PCR) Inv22 diagnostic tests revealed that these patients carried either type I or II Inv22. However, they showed a wild-type (WT) pattern in the IS-PCR Inv22 complementary tests. We further analyzed their X chromosomes to account for the puzzling results, and found that they had different centromeric breakpoints in the Inv22 X chromosomes, adjacent to the palindromic regions containing *int22h*-2 or -3, and their spacer region, respectively. The connections appeared to be shifted towards the telomere of the WT *F8* Xq28, resulting in a new telomere with an additional intact *int22h* copy. *Conclusions:* These gene rearrangements might result from double-strand breaks in the most distal regions of the long arms of the Inv22 X chromosomes, followed by DNA restorations using the WT *F8* Xq28 by non-homologous end joining or break-induced replication; thus leading to large *F8* deletions in severe hemophilia A patients.

Correspondence: Tetsuhito Kojima, Department of Pathophysiological Laboratory Sciences, Nagoya University Graduate School of Medicine, 1-1-20, Daiko-Minasmi, Higashi-ku, Nagoya 461-8673, Japan.
Tel.: +81 52 719 3153; fax: +81 52 719 3153.
E-mail: kojima@met.nagoya-u.ac.jp

Received 22 March 2012, accepted 31 July 2012



**Keywords**: deletion, *F8*, gene rearrangement, intron 22 inversion, inverse shifting-PCR, X chromosome.

## Introduction

Hemophilia A (HA) (OMIM 306700), the most common severe coagulation disorder with an incidence of one in 5000 males worldwide, is caused by the absence or impaired activity of the coagulation factor (F)VIII resulting from various mutations of the FVIII gene (*F8*). This large gene, which has been mapped to the most distal region (Xq28) of the long arm of the X chromosome, comprises 26 exons spread over 186 kb.

An intron 22 inversion (Inv22) disrupting *F8* at intron 22 is found in about half of the severe HA patients [1,2]. Inv22 results from homologous recombination between the *int22h*-1 region within the *F8* locus and either *int22h*-2 (Inv22 type II) or *int22h*-3 (Inv22 type I), which lie approximately 400 kb distal to *F8* [3]. Previously, *int22h*-2 and -3 were believed to be in opposite orientation to *int22h*-1. However, new sequence data show that only *int22h*-3 is in the opposite orientation to *int22h*-1, whereas *int22h*-2 is in the same orientation [4]. The palindromic arrangement of *int22h*-2 and -3 is now thought to permit an inversion polymorphism that allows *int22h*-2 to be in the telomeric arm of the palindrome and in opposite orientation to *int22h*-1 [5]. Intron 1 inversion (Inv1) is also a common mutation of HA with about 5% prevalence in severe HA [6]. It results from a homologous recombination between two nearly identical 1-kb sequences, *int1h*-1 and -2 in opposite orientations, lying in intron 1 of *F8* and in a more telomeric region located about 140-kb upstream, respectively.

Although a genomic inversion normally does not result in gain or loss of DNA, unusual patterns observed in *int22h*-

related inversions have led to the hypothesis of concomitant deletions [7–9], which can be associated with an increased risk of developing FVIII-inactivating antibodies (inhibitors). In a study of the correlation between a high incidence of inhibitors and gene defects producing a severe phenotype, approximately 41% of hemophiliacs carrying a large deletion in *F8*, whereas only 21% of patients with recurrent *int22h*-related inversions developed FVIII inhibitors [10]. A variety of *F8* mutations (1492 unique mutations) causing HA have been reported, of which 171 involve deletions of over 50 bp (HAMSTeRs database; http://hadb.org.uk/). However, only 10% of these large deletions have been fully characterized at the nucleotide level.

In this study, we investigated gene abnormalities in three unrelated severe HA patients with high-titer inhibitors, and identified distinct X-chromosomal rearrangements with *F8*-intron 22 inversions. These gene rearrangements might result from double-strand breaks and repair of the DNA in the most distal regions of the long arms of the Inv22 X chromosomes, leading to Inv22-related large *F8* deletions.

## Methods

### *Patients and DNA samples*

Three unrelated Japanese patients (P1–P3) and P2 family members enrolled in this study that was approved by the Ethics Committee of the Nagoya University School of Medicine. The patients were affected by severe HA (FVIII: C < 1%) and anti-FVIII antibodies had developed after replacement therapy. The titer of inhibitors in Bethesda units and the clinical characteristics of the patients are given in Table 1. Some of the clinical features of the patients have been previously reported [11] and P1 was diagnosed with dwarfism. In the previous study [11], the patients have been shown to carry large deletions of the *F8* exons 1–22 (P1 and P2) or 2–22 (P3), using Southern blot analysis. Genomic DNA samples were isolated from all patients after written informed consents were obtained; isolation was carried out from peripheral blood leukocytes using phenol extraction as described previously [12].

### *FVIII gene inversion detection*

Relevant DNA nucleotide positions are indicated on GenBank accession NC_000023.10. A long range polymerase chain reaction (Long PCR) was performed using four primers (P, Q, A and B) as described previously by Liu *et al.* [13]. The PQ fragment (12 kb) was amplified from intact *int22h*-1 in a wild-type (WT) *F8* male, the PB and AQ fragments (11 kb) were from *int22h*-1/-3 or -1/-2 and *int22h*-3/-1 or -2/-1 in Inv22 males, and the AB fragment (10 kb) was from non-recombined extragenic homologs. PCR was performed in 20-μL reaction volumes containing 50 ng of genomic DNA using 0.4 U of KOD FX DNA polymerase (Toyobo Co., Ltd., Osaka, Japan). Thermocycling involved 25 cycles of denaturation at 98 °C for 10 s and annealing/extension at 68 °C for 15 min; cycling was preceded by 94 °C for 2 min and followed by 7 min at 68 °C. PCR products were visualized after 3 h of electrophoresis at 50 V in a 0.6% agarose H (Nippon gene Co., Ltd., Tokyo, Japan) gel stained with 1 μg $mL^{-1}$ ethidium bromide.

Inverse shifting-PCR (IS-PCR) was performed as described previously [14] with minor modifications. Genomic DNA (2 μg) was digested with 15 units of *Bcl*I according to the manufacturer's instructions (New England Biolabs Japan, Inc., Tokyo, Japan) for 4 h in 50 μL. DNA fragments were circularized using Ligation high ver. 2 (Toyobo Co., Ltd.) in 8 μL at 16 °C for 1 h and recovered in 30 μL of 10 mM Tris with 1 mM EDTA, pH 8.0 (TE buffer) after ethanol precipitation. PCR was performed in reactions containing 2 μL of circularized DNA, in the presence of 0.5 μM of each primer, 0.4 U of KOD FX DNA polymerase and additional standard PCR reagents in a total volume of 20 μL. We designed modified primers for IS-PCR (Table S1). Thermocycling involved 34 cycles of denaturation at 98 °C for 10 s, primer annealing at 66 °C for 30 s and extension at 68 °C for 40 s; cycling was preceded by 94 °C for 2 min, each two cycles of 98 °C for 10 s and 68–74 °C for 35 s, followed by 1 min at 68 °C. PCR products were analyzed by electrophoresis on a 2% agarose gel stained with 1 μg $mL^{-1}$ ethidium bromide.

### *PCR mapping to evaluate Xq28 deletions*

To confirm and further assess the extent of the deletions, primer pairs for PCR mapping were designed to amplify fragments of 184–514 bp in the reference sequence (Table S2). PCR reactions were performed using rTaq DNA polymerase (Toyobo Co., Ltd.) or KOD FX DNA polymerase at an annealing temperature of 52–68 °C and products were analyzed on a 2% agarose gel. As the patients had only one X chromosome, we were able to assess the deletion by the absence of amplified products.

**Table 1** Clinical characteristics and results of *F8* abnormalities of hemophilia A patients

| Patient | Age | Sex | FVIII:C (%) | Inhibitor titer (BU $mL^{-1}$) | Gene abnormality | |
|---|---|---|---|---|---|---|
| | | | | | Deletion[11] | Inv22 |
| P1 | 17 | M | < 1 | 100–4000 | Exons 1–22 | Atypical |
| P2 | 25 | M | < 1 | 180–4000 | Exons 1–22 | Atypical |
| P3 | 16 | M | < 1 | 24 | Exons 2–22 | Atypical |

### *Identification of deletion breakpoints in X chromosomes*

To amplify the unknown regions including the breakpoints, we performed inverse PCR using primer sets designed in opposite orientations in the respective known regions (Table S3). This procedure employs two thermal cycling reactions of nested PCR to amplify from a region of known sequence into an unknown area. First, we digested 100–200 ng of DNA with an appropriate restriction enzyme (*Ssp*I for P1, *Hin*dIII for P2, and *Bcl*I for P3) (New England Biolabs Japan, Inc., Roche Diagnostics K.K., Tokyo, Japan) at the appropriate temperature for each. DNA fragments were circularized using Ligation high ver. 2 and recovered in 5 μL of TE buffer after ethanol precipitation. PCR was performed in reactions containing 5 μL of circularized DNA in the presence of 0.5 μM of each primer, 0.4 U of KOD FX DNA polymerase and additional standard PCR reagents in a total volume of 20 μL.

For nested PCR, we designed two kinds of primers for each reaction (Table S3). PCR products were analyzed by electrophoresis on a 2% agarose gel stained with 1 μg $mL^{-1}$ ethidium bromide. Inverse PCR products were purified using QIAEX II (Qiagen, Tokyo, Japan) and DNA sequencing was performed as described previously [15]. Screened sequences were analysed by NCBI BLAST (http://blast.ncbi.nlm.nij.gov/Blast.cgi).

We also designed multiplex PCR primers located on both sides of the junctions to amplify across the breakpoints of the rearrangements (Table S4). We performed PCRs for the respective genomic DNAs from the patients, the family members of P2 (his mother and grandmother) and the WT male controls, followed by DNA sequencing.

## Results

### *Abnormal patterns in analyzes of F8 int22h-related inversions in severe HA patients*

As the HA patients had a severe phenotype, we investigated whether they carried the common *F8 int22h*-related inversion (Inv22). Long PCR confirmed an Inv22 by yielding the expected 11-kb AQ product for *int22h*-2/-1 or -3/-1; however, the absence of an amplification product with primers P and B indicated a deletion of the *int22h*-1/-2 or -1/-3 counterpart (Fig. 1).

In the IS-PCR diagnostic test for Inv22, P1 and P2 showed a 341-bp fragment of the Inv22 type I pattern; whereas, P3 showed a 419-bp fragment of the Inv22 type II pattern (Fig. 2A). In the Inv22 complementary test, all patients showed the 489- and 411-bp fragments as the WT pattern (Fig. 2B). In the diagnostic test for Inv1, all patients lacked bands (Fig. 2C).

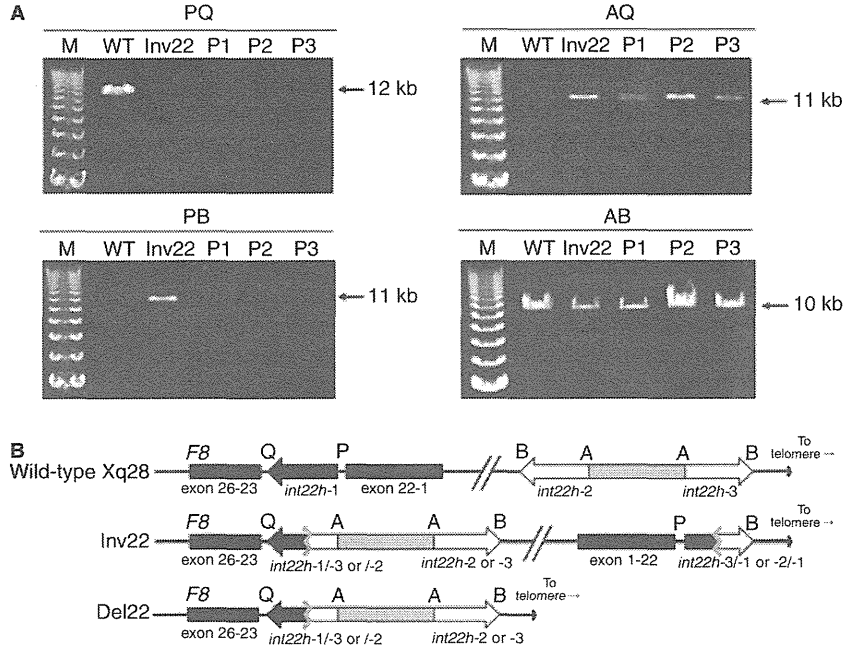


**Fig. 1.** Long PCR analysis for the *F8 int22h*-related inversion. (A) PCR products with primers PQ, PB, AQ and AB. The PQ fragment (12 kb) was amplified from intact int22h-1 in a wild-type (WT) *F8* male, the PB and AQ fragments (11 kb) were from int22h-1/-3 or -1/-2 and int22h-3/-1 or -2/-1, respectively, in an Inv22 male (Inv22) and the AB fragment (10 kb) was from non-recombined extragenic homologs. All patients (P1–P3) showed AQ products indicating Inv22 on the centromeric side; however, they lacked PQ products indicating a deletion of the telomeric-side counterparts of Inv22. M, 1 kb DNA ladder marker; WT, wild-type control; Inv22, HA patient with Inv22; P1, patient 1; P2, patient 2; P3, patient 3. (B) A scheme of the expected structures of the wild-type, Inv22, or Del22 X chromosomes along with long PCR primer sites.

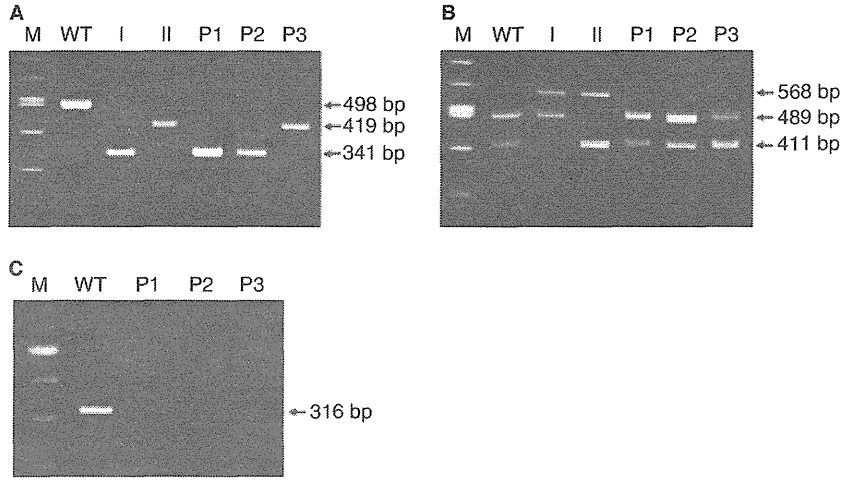


**Fig. 2.** Inverse shifting-PCR analysis of *F8*. (A) Inv22 diagnostic test: M, 100-bp DNA ladder marker; WT, wild-type control (498 bp); I, Inv22 type I control (341 bp); II, Inv22 type II control (419 bp); P1, patient 1; P2, patient 2; P3, patient 3. P1 and P2 show a 341-bp fragment as an Inv22 type I pattern, whereas P3 shows a 419-bp fragment as an Inv22 type II pattern. (B) Inv22 complementary test: WT, wild-type control (411 and 489 bp); I, Inv22 type I control (489 and 568 bp); II, Inv22 type II control (411 and 568 bp). All patients show 411 bp and 489 bp as the wild-type pattern. (C) Inv1 diagnostic test: WT, wild-type control (316 bp). The 281-bp fragment represents the Inv1 pattern. No patients show a band. The primer sequence data are given in Table S1.

### *PCR mapping to evaluate Xq28 deletions*

PCRs using 16 different primer pairs (A–P in Table S2) were mapped to confirm and further assess the extent of the deletions, given that previous Southern blot analysis had shown large deletions of *F8* in the patients [11]. In P1, primer pair K amplified a product but primer pair L did not, indicating that the centromeric breakpoint was located within the region defined by these two primer pair sets in the Inv22 type I X chromosome of the patient. Likewise, the centromeric ends of the deleted segments were localized between primer pairs M and F in the Inv22 type I X chromosome of P2, and O and P in the Inv22 type II X chromosome of P3, respectively (Fig. 3). The telomeric region products of primer pair J were amplified in all patients.

### *Identification of deletion breakpoints in X chromosomes*

From the results of PCR mapping, we roughly determined the centromeric ends of the deletion regions in the X chromosomes of the patients. We then employed inverse PCR followed by DNA sequencing to identify the centromeric and telomeric breakpoints.

In the case of the Inv22 type I X chromosome of P1, *Ssp*I sites were present at 1.1 kb on the centromeric side and 0.8 kb on the telomeric side of the primer pair K for PCR mapping, respectively (Fig. 4). Inverse PCR of the *Ssp*I-digested DNA of P1 failed to amplify the deduced 1.8-kb fragment and instead amplified an abnormal 2.2-kb fragment. Sequence data of the abnormal 2.2-kb fragment revealed a breakpoint located at nt 154 426 072 (GenBank accession NC_000023.10), about 20 kb on the telomeric side from *VBP1* on the Inv22 type I X chromosome. The adjacent telomere side sequences were located at nt 154 598 975 and nt 154 701 245 in the palindromic regions of *int22h*-2 and -3, respectively, in centromere direction in the Inv22 type I X chromosome; however, either one was in telomere direction in the WT *F8* X chromosome. There were three bases of microhomology (CTT) at the junction (Fig. 5, P1).

In the case of the Inv22 type I X chromosome of P2, *Hin*dIII sites were present at 0.8 kb on the centromeric side and 2.7 kb on the telomeric side of the primer pair M for PCR mapping, respectively (Fig. 4). Inverse PCR of the *Hin*dIII-digested DNA of P2 amplified a 2-kb fragment instead of the expected 3.3-kb fragment. The sequence of the abnormal 2-kb fragment contained a breakpoint located at nt 154 296 978 in *MTCP1* in the Inv22 X chromosome. The adjacent telomere side sequences were located at nt 154 566 155 and nt 154 734 058 in the palindromic regions of *int22h*-2 and -3, respectively, in a centromere direction in the Inv22 type I X chromosome; however, either one was in telomere direction in the WT *F8* X chromosome. There was one base of microhomology (C) at the junction (Fig. 5, P2).

In the case of the Inv22 type II X chromosome of P3, *Bcl*I sites were present at 3.3 kb on the centromeric side and 9.7 kb on the telomeric side of the primer pair O for PCR mapping. Inverse PCR of the *Bcl*I-digested DNA of P3 amplified a 5-kb fragment instead of the expected 12.6-kb fragment. The sequence of the abnormal 5-kb fragment contained a breakpoint located at nt 154 241 636 in *F8* intron 1. The adjacent telomere side sequence was located at nt 154 625 305 between the palindromic regions of *int22h*-2 and -3 in centromere direction in the Inv22 type II X chromosome; however, it was in telomere direction in the WT *F8* variant X chromosome, *int22h*-132 (according to the Xq- > Xtel orientation of *int22h*-1, -2, and -3 sequences) [16].

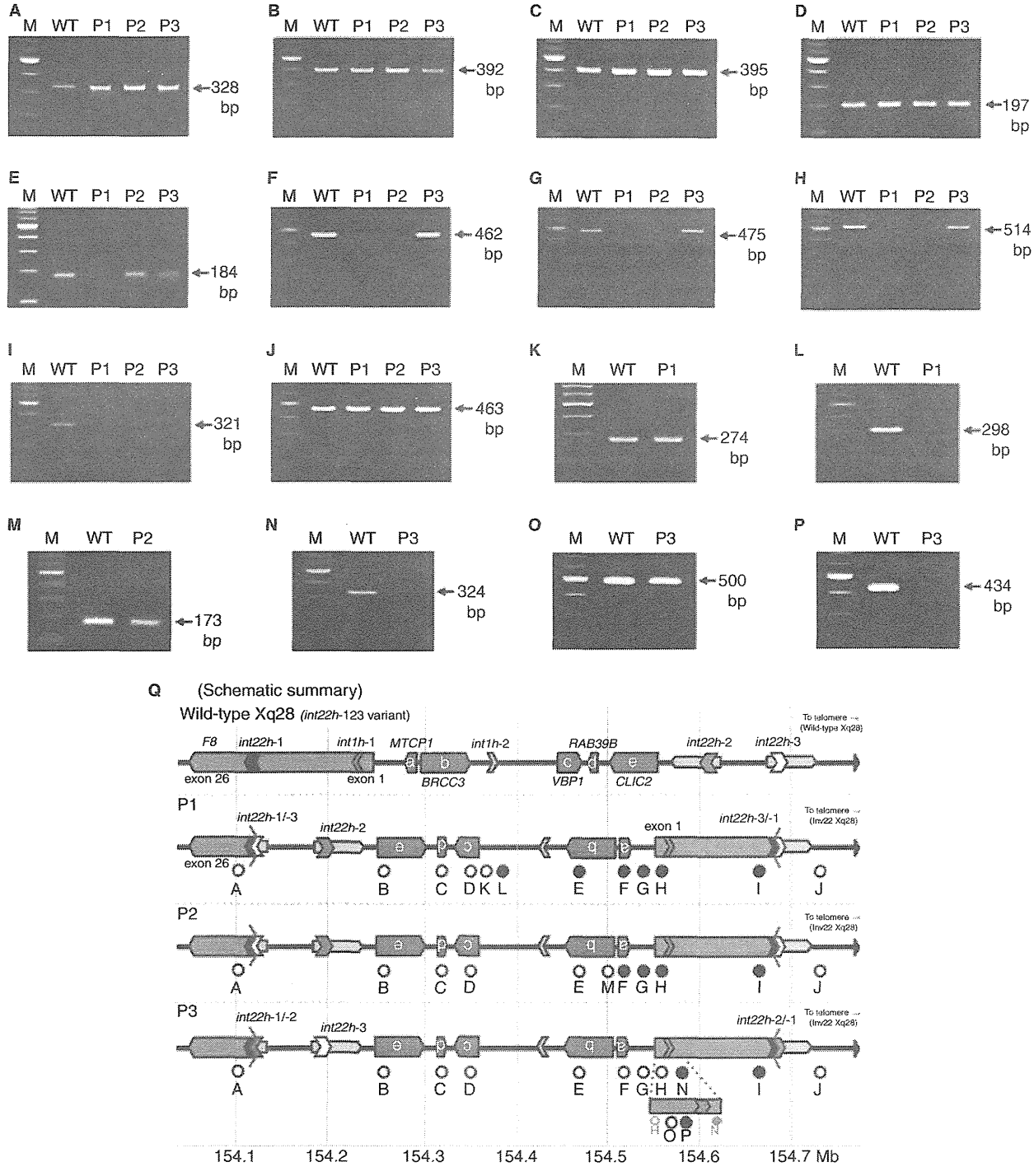


**Fig. 3.** PCR Mapping. (A–P) PCR mapping products separated on agarose gel electrophoresis for the determination of intact or deleted regions on the Xq28 of the patients. The presence of a PCR product in the patient indicates that the primer sequences are located in the intact region, and the absence of a product indicates that the primer sequences are located in the deleted region. Primer pair locations are shown below and primer sequence data are given in Table S2. M, the 100 bp ladder; WT, wild-type control male DNA; P1, patient 1; P2, patient 2; P3, patient 3. (Q) Schematic summary of PCR-mapped locations on Xq28 (NC_000023.10, 154.0–154.8 Mb). A–P indicate sites of PCR primer pairs. Open circles indicate the PCR amplified regions, and closed circles indicate the PCR failure regions. Salmon pink boxes, *F8*; closed chevrons, intragenic int22h-1; dark gray and open chevrons within the arms of a large imperfect palindrome (light grey), *int22h*-2 and -3, respectively; orange and yellow chevrons, *int1h*-1 and -2. Chimeric *int22h* sequences are denoted as [/] e.g., int22h-1/-2 represents the chimera between *int22h*-1 and -2. Five genes between *F8* and *int22h*-2, *MTCP1* (a), *BRCC3* (b), *VBP1* (c), *RAB39B* (d), and *CLIC2* (e) are shown as green boxes.

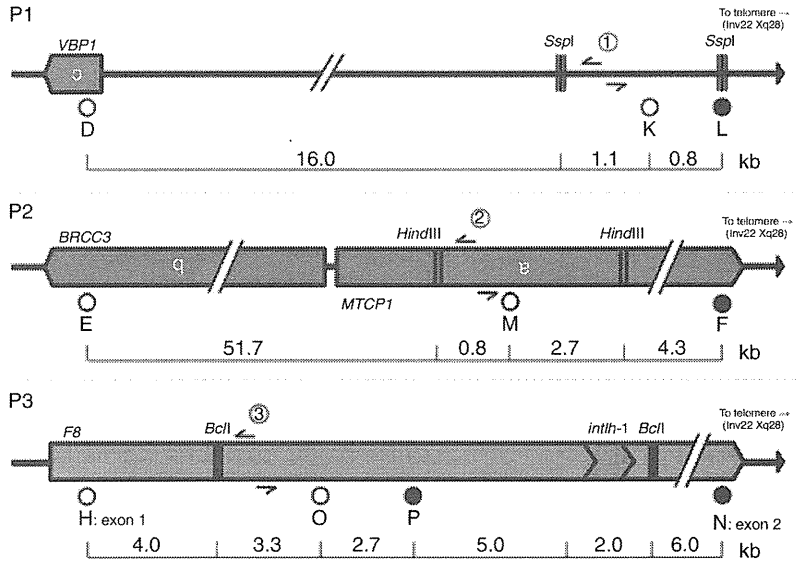


**Fig. 4.** Locations of restriction enzyme sites and inverse PCR primers used to identify the breakpoint junctions. Values indicate the sizes of regions in kb, whereas circled numbers (1–3) show the binding sites of primers used for inverse PCR to identify the breakpoints. Open and closed circles indicate the PCR-mapped regions of successful and failed amplifications, respectively. We used *Ssp*I for P1, *Hin*dIII for P2 and *Bcl*I for P3 in inverse PCRs to determine the breakpoint junctions, respectively. Schematic symbols are as in Fig. 3Q. Primer sequences are shown in Table S3.

There were no bases of microhomology at the junction (Fig. 5, P3).

All adjacent sequences of the breakpoints directed towards centromere in the Inv22 X chromosomes, P1 and P2 in type I, and P3 in type II, respectively. Whereas these sequences directed towards telomere in the WT *F8* X chromosomes, P1 and P2 in *int22h*-123 or -132 variant, and P3 in *int22h-132* variant, respectively (Fig. 5, bottom). The two WT Xq28 variants were as a result of a non-deleterious inversion polymorphism, which changed the relative positions and orientations of *int22h*-2 and -3 [3].

The putative breakpoint junctions were subsequently confirmed by the PCRs with primers located on both sides of the junctions. The patients (P1–P3) and the family members of P2 (his mother and grandmother) showed predicted PCR products, respectively, but the WT male control for each breakpoint did not (Fig. S1).

## Discussion

A variety of gene abnormalities, point mutations including nucleotide substitutions, small insertions/deletions and *F8*-related inversions causing HA have been reported. Large deletions in *F8* account for approximately 5% of HA, and almost all cases of gross DNA rearrangements result in low levels of FVIII: C < 1%, corresponding to clinically severe disease. We have described complex X-chromosome rearrangements in three unrelated Japanese patients affected with severe HA. In a previous study [11], the patients were shown to carry large deletions of the *F8* exons 1–22 (P1, P2) or 2–22 (P3), using Southern blot analysis; however, the precise gene abnormalities were not fully elucidated.

In the long PCR analyzes, all patients displayed expected AQ products resulting from centromeric recombination of the Inv22 X chromosome, but unexpectedly lacked PB products from its telomeric recombination. In the IS-PCR analyzes, Inv22 diagnostic tests showed that P1 and P2 had an Inv22 type I, whereas P3 had an Inv22 type II; however, they unexpectedly showed wild-type patterns in the complementary tests. These data indicated that the patients carried an inversion *int22h* copy on the centromeric side but not on the telomeric side, and thus could carry an intact *int22h* copy in the most telomeric region. Thus, abnormal rearrangements might be combined with Inv22 in the terminal end of the long arm of the X chromosomes of these patients.

We hypothesized that the patients carried Inv22 and large *F8* deletions in the terminal region of the long arms of their X chromosomes. Accordingly, we investigated the X chromosomes of the patients by PCR mapping, inverse PCR and DNA sequencing to evaluate the deleted regions and their breakpoints. In PCR mapping, we could roughly estimate the locations of the centromeric ends of the deleted segments in the Inv22 X chromosome. Subsequent inverse PCR and DNA sequencing revealed their deletion breakpoints. The sequences of the telomeric ends of the breakpoints in P1 and P2 were found in palindromic arms of *int22h*-2 or -3, each allowing two possible positions, whereas the telomeric ends of the breakpoints in P3 were found between the palindromic regions of *int22h*-2 and -3. All adjacent sequences were directed towards the centromere in the Inv22 X chromosomes, resulting in loss of telomere structures. If the deletion took place after Inv22, the DNA restoration after double-strand breaks (DSBs) using a WT *F8* Xq28 variant, *int22h*-123 or *int22h*-132, could make a breakpoint followed in matching direction towards a telomere

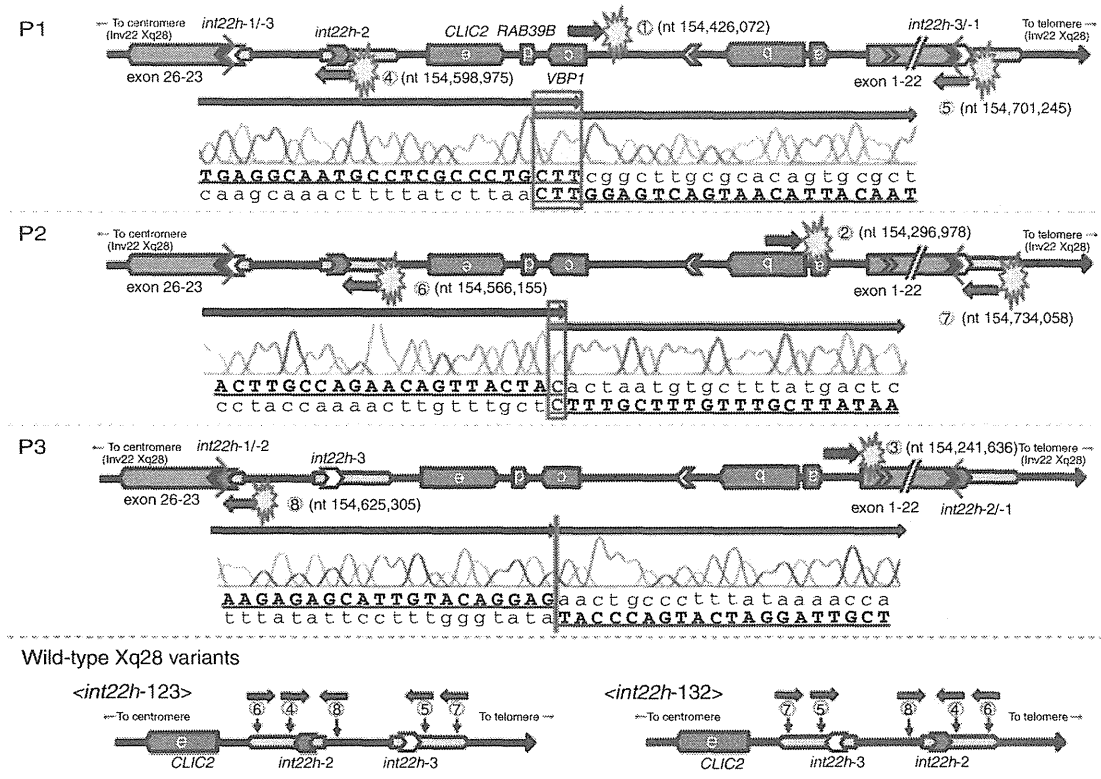


**Fig. 5.** DNA sequencing electropherograms of fragment breakpoint junctions. Sequence orientations are indicated by purple (centromeric side) and red (telomeric side) arrows. Breakpoint candidates are indicated by starburst symbols along with circled numbers. Schematic symbols are as in Fig. 3Q. (P1) The junction in Xq28 of P1 is located at nt 154 426 072 (the nucleotide position is with reference to the wild-type (WT) X chromosome: GenBank accession NC_000023.10), about 20 kb on the telomeric side from *VBP1* on the Inv22 type I X chromosome. The adjacent telomere side sequences are located at nt 154 598 975 and nt 154 701 245 in the palindromic regions of *int22h*-2 and -3, respectively, in centromere direction in the Inv22 type I X chromosome. The CTT in the boxed sequence indicates an overlapping sequence common to both regions. (P2) The junction in Xq28 of P2 is located at nt 154 296 978 in *MTCP1* of the Inv22 type I X chromosome. The adjacent telomere side sequences are located at nt 154 566 155 and nt 154 734 058 in the palindromic regions of *int22h*-2 and -3, respectively, in centromere direction in the Inv22 type I X chromosome. A cytosine residue common to both sequences is boxed. (P3) The junction in Xq28 of P3 is located at nt 154 241 636 in *F8* intron 1, adjacent to nt 154 625 305 between the palindromic regions of *int22h*-2 and -3 proximally in the Inv22 type II X chromosome. There are no bases of microhomology at the junction. (WT Xq28 variants) Positions and directions of telomere side sequences of the breakpoints are plotted on the two WT *F8* variants Xq28, *int22h*-123 and -132 (according to the Xq- > Xtel orientation of the *int22h*-1, -2, and -3 sequences). Circled numbers correspond to the positions in the Inv22 X chromosomes of the patients. In the two WT variants Xq28, each adjacent telomere side sequence of the breakpoints found in the patients directed towards a telomere at least in one position.

as shown in Fig. 5 (bottom). It is well known that the telomere structure of the chromosome is essential for the cell to survive. Therefore, the DNA DSBs would be repaired with a WT X chromosome to regain a telomere structure, resulting in the presence of one more additional intact *int22h*-2 or -3 as detected in the IS-PCR (Fig. 2B). These complex abnormalities could be caused by repair mechanisms after DNA DSBs.

DSBs are potentially lethal lesions that occur spontaneously during normal cell metabolism or upon treatment of cells with DNA-damaging agents. There are two major mechanisms for repairing DSBs: non-homologous end joining (NHEJ) and homologous recombination (HR). NHEJ involves the religation of the two ends of the broken chromosome and can occur with high fidelity, or be accompanied by gain or loss of nucleotides at the junction [17,18]. NHEJ occurs intra- or interchromosomally and can lead to a small deletion, insertion, or indel or a large deletion or inversion in the first case and a translocation in the second case. HR relies on the presence of a homologous duplex as a template for repair of the broken chromosome [19]. Several sub-pathways of HR have been defined, including DSB repair, synthesis-dependent strand annealing and break-induced replication (BIR). BIR, which has been experimentally observed in yeast, might also be capable of causing complex rearrangements in humans leading to HA [20]. The microhomologies identified at the breakpoints of human complex rearrangements are not sufficiently long to be employed in classic BIR. Replication-based mechanisms can readily explain complex rearrangements and the microhomologies at breakpoints. However, breakpoint sequence analyzes of complex rearrangements also show in some cases an absence of microhomology, which could indicate NHEJ-specific nucleotide insertion or deletion [21].

These rearrangements might not occur simultaneously, because most instances of Inv22 occur during spermatogenesis [22], and a chromosome pair is needed to repair DSB. We deduced that in the studied families, first Inv22 occurred during

spermatogenesis and then a DSB occurred on the maternal X chromosome with Inv22, followed by repair by NHEJ and/or BIR during oogenesis. Incidentally, P2's mother and grandmother carried in the heterozygous state the same mutation as in P2 (Fig. S1B), suggesting that this rearrangement was inherited over the generations.

Several independent reports using Southern blot and long PCR analyzes have shown unusual patterns with both *int22h*-related inversion and deletion of *F8* causing severe HA ('rare inversion type') [8,23,24], and we identified three such cases in our study. So far, we identified three such large deletions in 63 severe HA patients tested for Inv22 in our laboratory, these deletions could be missed using any of the standard Southern blot or PCR approaches to analyze the Inv22.

As one of the precedents for DNA repair, Sheen *et al.* [20] reported a complex mutational event resulting from DNA repair that incorporates BIR and serial replication slippage in a severe HA patient. That mutational event consisted of two adjacent complex deletion/insertions; one involving a deletion of the promoter and exon 1 of *F8*, and the other involving a large deletion/insertion that removes the entire coding sequence of the *FUNDC2* gene. Moreover, they found a large duplication of four genes (*TMEM185A*, *HSFX1*, *MAGEA9* and *MAGEA11*) in the latter deletion/insertion. They concluded that this complex genomic rearrangement was generated by two distinct, but linked, repair mechanisms in response to simultaneous DSB. Although the complex rearrangement by a combination of complex deletions and insertions was not found in our three cases, it is suggested that the combination of DNA DSB and a repair mechanism in the telomere region of the Inv22 X chromosome might be less rare than supposed.

Five genes between *F8* and *int22h*-2 used as markers in this study are well characterized on Mendelian Inheritance in Man: *MTCP1* (OMIM 300116), *BRCC3* (OMIM 300617), *VBP1* (OMIM 300133), *RAB39B* (OMIM 300774) and *CLIC2* (OMIM 300138). In this study, P1 carried the largest deletion of about 270 kb including *F8* exons 1–22, *MTCP1* and *BRCC3*. Recently, Miskinyte *et al.* [25] reported that a loss of *BRCC3* led to abnormal angiogenesis and was associated with X-linked moyamoya syndrome, which is characterized by the association of a moyamoya angiopathy, short stature and a stereotyped facial dysmorphism. They investigated families affected by X-linked syndromic moyamoya disorder, in which an overlapping deletion at Xq28 removed *MTCP1* and *BRCC3* and cosegregated with the affected phenotype. Very interestingly, P1 in our study had a facial dysmorphism and short stature, and was diagnosed with dwarfism. In view of the findings of Miskinyte *et al.*, the short stature of P1 could be as a result of the deletion of *BRCC3*.

In conclusion, we identified three distinct gene rearrangements in the most distal region of the long arm of the Inv22 X chromosome that appeared to result from DSB-BIR (and/or -NHEJ) DNA repair, leading to large *F8* deletions in severe HA patients with high responding FVIII inhibitors. Elucidation of such complex gene rearrangements will help to understand the molecular mechanism behind not only gross X chromosomal rearrangements causing severe HA, but also genomic rearrangements causing other genetic diseases.

## Addendum

J. Fujita and Y. Miyawaki contributed equally to this work, sharing first authorship, and designed and performed the research, analyzed the data and drafted the manuscript; A. Suzuki, A. Maki, E. Okuyama and M. Murata performed experiments, analyzed the data and contributed analytic methodology; A. Takagi and T. Murate contributed analytic methodology and analyzed the data; T. Matsushita and N. Suzuki developed the project, collected and analyzed the clinical data; H. Saito supervised the project and edited the manuscript; and T. Kojima designed the project, analyzed data and wrote the manuscript.

## Acknowledgements

We wish to thank C. Wakamatsu for her excellent technical assistance. This study was supported in part by grants-in-aid from the Japanese Ministry of Education, Culture, Sports, Science, and Technology (2259524) (T.K.), the Japanese Ministry of Health, Labour and Welfare (Research on Measures for Intractable Diseases) (T.K.) and the Baxter Hemophilia Foundation (Y.M.). The authors would like to thank Enago for the English language review.

## Disclosure of Conflict of Interest

The authors state that they have no conflict of interest.

## Supporting Information

Additional Supporting Informationmay be found in the online version of this article:

**Figure S1.** Rearrangement specific PCR of the patients and the family members of P2.
**Table S1.** (A) IS-PCR primers. (B) Expected product size in each reaction.
**Table S2.** PCR mapping primers.
**Table S3.** Inverse PCR and sequencing primers.
**Table S4.** Breakpoint specific primers.

Please note: Wiley-Blackwell are not responsible for the content or functionality of any supporting materials supplied by the authors. Any queries (other than missing material) should be directed to the corresponding author for the article.

## References

1 Lakich D, Kazazian HH, Antonarakis SE, Gitschier J. Inversions disrupting the factor VIII gene are a common cause of severe haemophilia A. *Nat Genet* 1993; 5: 236–41.